Properties of steady-state in Er^{3+}-Yb^{3+} co-doped phosphate glass for optical waveguide laser

Yuxi Liu (刘玉喜)[1], Xiaoxia Zhang (张晓霞)[1], Ying Li (李 瑛)[1], and Ying Pang (庞 莹)[2]

[1]*School of Optic-Electronic Information, University of Electronic Science and Technology of China, Chengdu 610054*

[2]*School of Communication and Information Engineering, University of Electronic Science and Technology of China, Chengdu 610054*

Received November 10, 2006

Transitions of laser diode (LD) pumped Er^{3+}-Yb^{3+} co-doped glass laser are rather complicated. Considering energy transfer between Er^{3+} and Yb^{3+} ions, cross-relaxation, upconversion luminescence, and other transition processes, rate equations of quasi-three energy-level-system of the Er^{3+}-Yb^{3+} co-doped laser are presented. The output characteristics are also calculated and analyzed in detail. The results show that Er^{3+}-Yb^{3+} co-doped phosphate waveguide lasers with high slope efficiency and low threshold can be achieved.

OCIS codes: 140.3500, 140.3580, 140.3380.

Erbium laser glass has been the subject of many investigations in recent years. This is mostly due to the erbium ions fluorescence transition around 1.5 μm, which is very suitable for applications in eye-safe range finding[1] and long-range optical fiber communications. Since the efficiency of direct pumping of Er^{3+} in glasses is low, co-doping with additional sensitizer ions is usually required[2,3]. The most common sensitizer ion is Yb^{3+}, which strongly absorbs with transition into a broad $^2F_{5/2}$ band and transfers the energy to the $^4I_{11/2}$ manifold of Er^{3+} by a non-radioactive cross-relaxation process[4].

In this paper, we present a characteristic procedure to determine the most of the waveguide relevant parameters. The Er^{3+}-Yb^{3+} co-doping system in phosphate glass is analyzed in detail and the determined characteristic parameters are studied. Phosphate glass is excellent for rare-earth host materials and the ytterbium co-doping offers the advantage of a large absorption cross section near 980 nm and a good spectral overlap of its emission with the erbium absorption, leading to an efficient energy transfer from ytterbium to erbium[3]. We also analyze the transition of the ions and rate equations of quasi-three-level-system. The numerical method for calculation is also analyzed.

Phosphate glasses are known to be excellent for rare-earth host materials in terms of their spectroscopic characteristics, and have been widely used for bulk laser applications. The high Er^{3+} doping concentrations $> 10^{26}$ m^{-3} that are required in order to achieve the high gain within a few centimeters of length (that the integrated optics active components need) can be doped into phosphate glass without serious ion clustering because of their high solubilities for rare-earth ions[3]. However, the pumping efficiency of the active devices is seriously limited because of the relatively low absorption cross section of Er^{3+} for the usual pumping wavelengths. This pumping efficiency can be enlarged by co-doping Yb^{3+}. Figure 1 shows the schematic energy-level diagram of an Er^{3+}-Yb^{3+} co-doped system in phosphate glasses for amplification in 1.5 μm and considering a 980-nm pump wavelength[4].

The rate equations for this system, which describe the temporal evolution of the population densities of the levels in the materials populated and depleted by absorption, stimulated emission, spontaneous emission, and other transition processes shown in Fig. 1, can be written as[4,5]

$$\frac{\partial n_1}{\partial t} = -W_{12}n_1 + W_{21}n_2 + Cn_2n_3, \tag{1}$$

$$\frac{\partial n_3}{\partial t} = -W_{35}n_3 - W_{34}n_3 + W_{43}n_4 + A_{43}n_4 + C_{44}n_4^2 - Cn_2n_3, \tag{2}$$

$$\frac{\partial n_4}{\partial t} = W_{34}n_3 - A_{43}n_4 - W_{43}n_4 + S_{54}n_5 - 2C_{44}n_4^2, \tag{3}$$

$$\frac{\partial n_5}{\partial t} = W_{35}n_3 - S_{54}n_5 + A_{65}n_6 + Cn_2n_3, \tag{4}$$

$$\frac{\partial n_6}{\partial t} = C_{44}n_4^2 - A_{65}n_6, \tag{5}$$

$$n_1 + n_2 + n_3 + n_4 = N_1, \tag{6}$$

$$n_5 + n_6 = N_2, \tag{7}$$

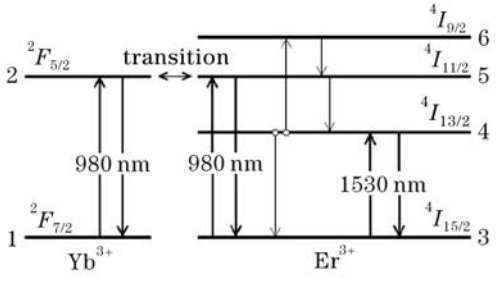

Fig. 1. Energy level scheme of the Er^{3+}-Yb^{3+} co-doping system in a phosphate glass.

1671-7694/2007/070418-04

where the population densities of the erbium levels $^4I_{15/2}$, $^4I_{13/2}$, $^4I_{11/2}$, and $^4I_{9/2}$ and of the ytterbium levels $^2F_{7/2}$ and $^2F_{5/2}$ are represented by $n_1(x,y,z)$, $n_2(x,y,z)$, $n_3(x,y,z)$, $n_4(x,y,z)$, $n_5(x,y,z)$, and $n_6(x,y,z)$, respectively. Moreover, the z-independent erbium and ytterbium concentration profiles are denoted as N_1 and N_2. In Eqs. (1)−(7), A_i represents the spontaneous relaxation rate, whereas C_{44} is the homogeneous up-conversion coefficient and C is the energy transfer coefficient.

Some realistic values provided by the waveguide supplier or taken from literatures are used as the initial values of the characteristic parameters for our computation. We also made a few reasonable assumptions as follows.

The values of densities of stimulated radiance can be obtained by[6]

$$W_{ij}(x,y,z) = \sum_v \frac{\sigma_{ij}(\nu)}{h\nu}\Psi(x,y,v) \times P(z,v), \qquad (8)$$

where $\Psi(x,y,z)$ is the normalized intensity distribution of the pump, signal or amplified spontaneous emission (ASE) waves, which depends on the waveguide geometry and index profile and is assumed to be z-independent, and $P(z,v)$ is the total optical power. $\sigma_{ij}(\nu)$ are the cross sections corresponding to the transition between the ith and jth levels. Note that in Eqs. (1) − (7), the spatial dependence of the population densities and those of the densities of stimulated radiance are omitted for simplicity.

We assume that McCumber theory is fully applicable for this system[6]. Therefore, emission cross sections $\sigma_e(\nu)$ can be obtained from the absorption cross sections $\sigma_\alpha(\nu)$ by using McCumber relation

$$\sigma_e = \sigma_\alpha(\nu)\exp(\frac{\varepsilon_T - h\nu}{kT}), \qquad (9)$$

which was demonstrated to be applicable to rare earth ions[6].

The mode intensity profiles are assumed to be Gaussian and have 5- and 6-μm diameters for 980- and 1534-nm wavelengths, respectively. These data were also provided by the waveguide supplier.

The waveguide supplier indicated that propagation losses were lower than 0.1 dB/cm at 1.5 μm. Insertion losses are evaluated from the waveguide and pigtail-fiber mode intensity profile diameters (3.94- and 5.86-μm diameters for 980- and 1534-nm wavelengths, respectively) to be negligible for the signal wavelength and 0.12 dB for 980 nm.

For simplicity, the same mode intensity profile and scattering losses for the signal wavelength can be assumed for all the wavelengths in the 1.5-μm ASE band, without any noticeable effect in the results. Other parameters used for numerical calculations are listed in Table 1.

It is indicated that changing Er^{3+} concentrations could lead to the changes of both slope efficiency and threshold simultaneously, as shown in Fig. 2. Numerical calculations indicate that the output powers can reach several tens of milliwatts, with the high slope efficiency near 20% and the threshold only about several milliwatts. The relationship between the output power and Er^{3+} concentration is shown in Fig. 3. We can see the phenomenon of the pump power bleaching with the low Er^{3+} concentration because the short waveguide length leads to the saturation of the output power. We know that the output power is a function of the slope efficiency and threshold, $P_{out} = \eta_s(P - P_{th})$. From Fig. 2, as the Er^{3+} concentration increases, the value of the slope efficiency becomes bigger and bigger with the step slowing down. When the concentration grows up to some point, it seems that the efficiency increases no more as the concentration increasing. We can conclude that some value of the density is optimum. Usually, the optimum concentration is a function of output coupler's optical transmission, medium length, and other parameters.

Table 1. Initial Values for Numerical Calculations

$\alpha(1534)$	8.3×10^{-2} dB/cm	C_{44}	8×10^{-25} m^3/s
C	1.8×10^{-23} m^3/s	ε_T	6514.7 cm^{-1}
c	3×10^{8} m/s	μ	6.63×10^{34} J·s
τ_e	8 ms	λ_p	980 nm
A_{21}	$1/(1.1\times10^{-3})$ s^{-1}	A_{43}	3.4×10^{5} s^{-1}
A_{65}	$1/(1.1\times10^{-3})$ s^{-1}	$\sigma_{12}(980)$	5.4×10^{-25} m^2
$\sigma_{21}(980)$	7.0×10^{-25} m^2	$\sigma_{35}(980)$	1.6×10^{-25} m^2
$\sigma_{53}(980)$	1.2×10^{-25} m^2	$\sigma_{34}(1534)$	5.4×10^{-25} m^2
$\sigma_{43}(1534)$	5.3×10^{-25} m^2	n	1.521

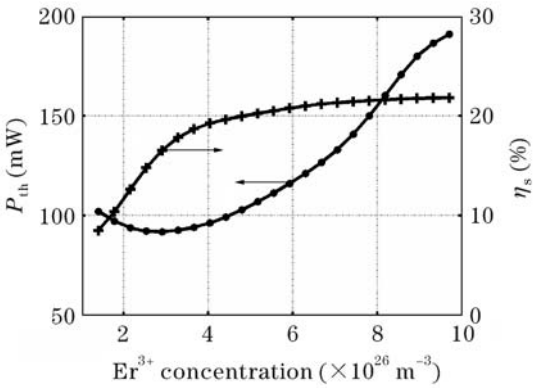

Fig. 2. Threshold and slope efficiency versus Er^{3+} concentration.

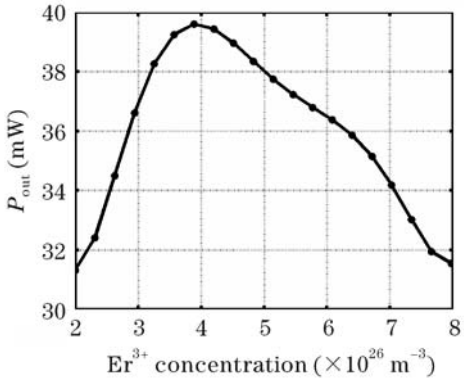

Fig. 3. Relationship between output power and Er^{3+} concentration.

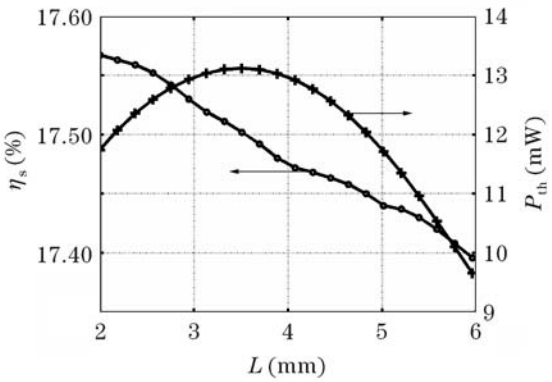

Fig. 4. Slope efficiency and threshold versus cavity length.

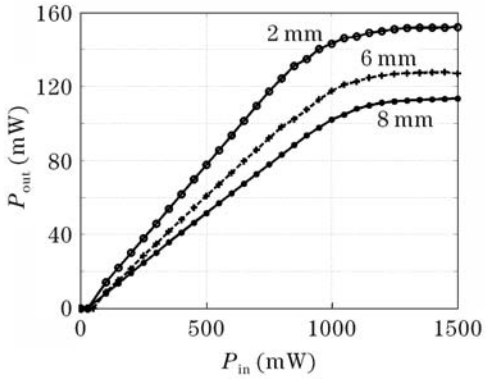

Fig. 5. Output power as a function of the pump power with different cavity lengths.

Changing cavity lengh not only leads to the changes of the oscillating laser waist but also influences other parameters such as the lifetime of photons in the cavity. Thereby changing cavity length will alter both threshold and slope efficiency, as shown in Fig. 4. After choosing the curvature radius of the output coupler, shorter cavity length will bring a lower threshold and a higher slope efficiency. Changes of the threshold and slope efficiency will affect the output power finally. Figure 5 shows the relationship between the output power and pump power. The output power becomes saturated when the pump power is high enough (about 900 mW). In the figure, we can see that the output power is highly sensitive to cavity length. When designing Er^{3+} and Yb^{3+} co-doped phosphate waveguide lasers and optimizing the relevant parameters, the cavity length is a crucial parameter. The values of other parameters for numerical calculations are $Er^{3+} = 2 \times 10^{26}$ m^{-3}, $l = 1.5$ mm, $T = 1.3\%$, and $w_0 = w_p = 50$ μm (w_0 is the oscillating laser waist, w_p is the pump laser waist in the medium).

Figure 6 shows the changes of slope efficiency and threshold with effects of output coupler's optical transmission. The relationship between the output power and transmission is shown in Fig. 7. Further analyses indicate that different optical transmissions of output couplers result in different losses in the cavity, which lead to the changes of output power. In Fig. 7, we can see that only some values of the transmission could bring the highest output power. Figure 7 also shows that the optimal transmission of output coupler becomes lower as the input power increases, which is very important

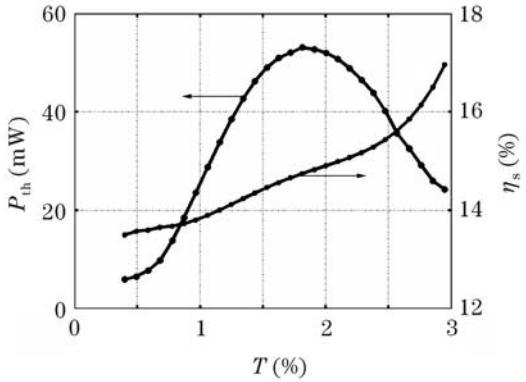

Fig. 6. Threshold and slope efficiency versus output coupler's transmission.

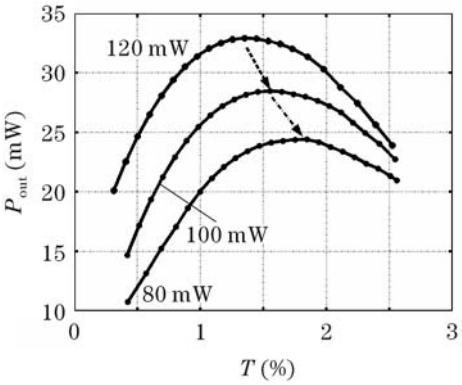

Fig. 7. Output power as a function of the output coupler's transmission with different pump powers.

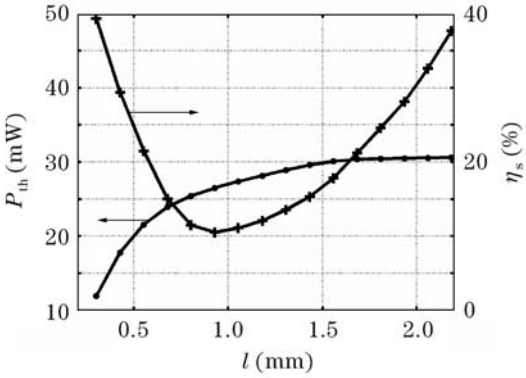

Fig. 8. Threshold and slope efficiency versus medium length.

for improving the laser's performance and optimizing the design of laser.

It is shown in Fig. 8 that the slope efficiency gets higher with the increase of the medium length and the increasing step becomes small enough to be neglected when the medium length reaches some point. But the relationship between the threshold and the medium length is highly subtle. The threshold is very high when the medium length is not long enough, and as the medium length increases the threshold decreases rapidly to its lowest point, from which it grows up slowly. We define the optimal length as the length of the medium at which the threshold is the lowest, it is a function of Er^{3+} concentration. Figure 9 shows the output power as a function of the medium

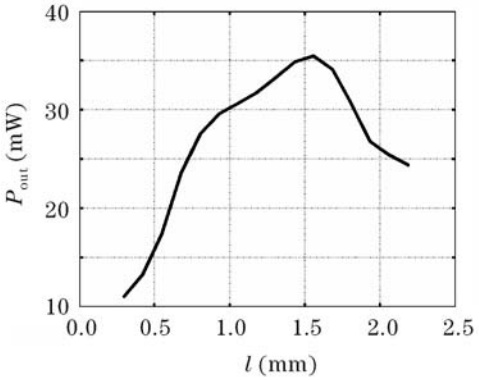

Fig. 9. Output power as a function of the medium length with the pump power of 220 mW.

length with the pump power of 220 mW. The optimal length gets shorter as the Er^{3+} concentration increases, and calculation indicates that the optimal length is independent of the pump laser waist in the medium.

In situ characterization techniques for waveguides that are not transversely accessible require both precise measurements of the in-out-coupled optical powers and a detailed model that incorporates all the mechanisms affecting the evolution of these optical powers along the active waveguide. When both requirements are fulfilled, most of the parameters can be determined by following a fitting procedure that has taken into account how relevant is each parameter influencing on the propagation of the different optical powers, and the performance of the waveguide for different applications can be accurately predicted. There is a good agreement between the obtained results and manufacturer's and published data.

This work was supported by the National Natural Science Foundation of China under Grant No. 90201011, 10174057. Y. Liu's e-mail address is yxliu428@163.com.

References

1. H. Chen, Y. Liu, J. Dai, Y. Yang, and Z. Guan, Acta Opt. Sin. (in Chinese) **23,** 697 (2003).
2. F. Song, X. Chen, Y. Feng, M. Shang, W. Zhang, G. Zhang, S. Jiang, and M. J. Myers, Chin. J. Lasers (in Chinese) **26,** 790 (1999).
3. M. Zhu and T. Gu, in *4th International Conference on Microwave and Millimeter Wave Technology Proceedings* 432 (2004).
4. J. A. Vallés, M. A. Rebolledo, and J. Cortés, IEEE J. Quantum Electron. **42,** 152 (2006).
5. X. Zhang, W. Pan, and Y. Liu, Proc. SPIE **4918,** 30 (2002).
6. Z. Liu, L. Hu, S. Dai, C. Qi, Z. Jiang, Acta Opt. Sin. (in Chinese) **22,** 1129 (2002).